Published in final edited form as:
*Exp Eye Res*. 2008 January ; 86(1): 81–91. doi:10.1016/j.exer.2007.09.011.

# Expression of Kir7.1 and a Novel Kir7.1 Splice Variant in Native Human Retinal Pigment Epithelium

**Dongli Yang**[a], **Anuradha Swaminathan**[a], **Xiaoming Zhang**[a], and **Bret A. Hughes**[a,b]

a *Department of Ophthalmology and Visual Sciences, University of Michigan, W.K. Kellogg Eye Center, 1000 Wall St., University of Michigan, Ann Arbor, MI 48105, USA*

b *Department of Molecular and Integrative Physiology, University of Michigan, Ann Arbor, MI 48009, USA*

## Abstract

Previous studies on bovine retinal pigment epithelium (RPE) established that Kir7.1 channels compose this epithelium's large apical membrane $K^+$ conductance. The purpose of this study was to determine whether Kir7.1 and potential Kir7.1 splice variants are expressed in native adult human RPE and, if so, to determine their function and how they are generated. RT-PCR analysis indicated that human RPE expresses full-length Kir7.1 and a novel Kir7.1 splice variant, designated Kir7.1S. Analysis of the human Kir7.1 gene (*KCNJ13*) organization revealed that it contains 3 exons, 2 introns, and a novel alternative 5′ splice site in exon 2. In human RPE, the alternative usage of two competing 5′ splice sites in exon 2 gives rise to transcripts encoding full-length Kir7.1 and Kir7.1S, which is predicted to encode a truncated protein. Real-time PCR indicated that Kir7.1 transcript is nearly as abundant as GAPDH mRNA in human RPE whereas Kir7.1S transcript expression is 4-fold lower. Western blot analysis showed that the splice variant is translated in *Xenopus* oocytes injected with Kir7.1S cRNA and revealed the expression of full-length Kir7.1 but not Kir7.1S in adult human RPE. Co-expression of Kir7.1 with Kir7.1S in *Xenopus* oocytes had no effect on either the kinetics or amplitude of Kir7.1 currents. This study confirms the expression of Kir7.1 in human RPE, identifies a Kir7.1 splice variant resulting in predicted changes in protein sequence, and indicates that there no functional interaction between this splice variant and full-length Kir7.1.

### Keywords

gene expression; potassium channels; splice variant; *KCNJ13*

## 1. Introduction

Potassium ($K^+$) channels in the RPE have a large impact on the rate and direction of ion, metabolite, and fluid transport between the subretinal space and choroid. They do so by influencing the membrane potential, a major factor determining the driving force on ion and solute flux through various channels and electrogenic cotransporters, and also by mediating $K^+$ secretion across the apical membrane, which is essential to subretinal $K^+$ homeostasis as well as $Na^+/K^+$ pump and Na,K,2Cl cotransporter function. Electrophysiological studies have

Corresponding author: Bret A. Hughes, W.K. Kellogg Eye Center, Department of Ophthalmology and Visual Sciences, University of Michigan, 1000 Wall Street, Ann Arbor, MI 48105-0714, USA, E-mail: E-mail: bhughes@umich.edu, Tel: 734-763-3738, Fax: 734-936-3815.

established that inwardly rectifying $K^+$ (Kir) channels comprise a major component of the RPE apical membrane $K^+$ conductance (Hughes and Steinberg, 1990; Hughes et al., 1995; Hughes and Takahira, 1996; Hughes and Takahira, 1998; Shimura et al., 2001; Yuan et al., 2003).

Kir channel subunits are a widely expressed group of structurally related proteins that co-assemble to form functional homotetrameric or heterotetramic channels (Isomoto et al., 1997). Each Kir channel subunit is composed of two transmembrane α helices, M1 and M2, separated by a conserved pore loop (H5) that forms the selectivity filter. Molecular cloning has led to the identification of fifteen Kir subtypes, most of which form $K^+$ channels with various degrees of inward rectification when expressed in heterologous expression systems.

Kir7.1, an inwardly rectifying $K^+$ channel with unusual permeation properties, was initially localized in epithelial cells of the thyroid, small intestine, kidney tubules, choroid plexus (Nakamura et al., 1999; Nakamura et al., 2000; Ookata et al., 2000). Later, Kir7.1 was found to be expressed in bovine and rat retinal pigment epithelium (RPE) (Kusaka et al., 2001; Shimura et al., 2001; Yang et al., 2003; Yuan et al., 2003), where it forms a major component of the apical membrane $K^+$ conductance (Shimura et al., 2001; Yang et al., 2003; Yuan et al., 2003). Native human RPE cells also exhibit a Kir current with properties consistent with Kir7.1 (Hughes and Takahira, 1996).

In the present study, we sought to confirm the expression of Kir7.1 in native human RPE and to determine whether Kir7.1 splice variants might also be expressed. We find that in addition to Kir7.1, human RPE expresses mRNA encoding a novel alternative splice variant of Kir7.1, designated Kir7.1S. We carried out molecular, biochemical, bioinformatic, and electrophysiological analyses to characterize the genomic organization of the human Kir7.1 gene (*KCNJ13*), assess Kir7.1 and Kir7.1S expression at the transcript and protein levels, and test for function interaction between the two splice variants. Some of these data have been reported in abstract form (Yang and Hughes, 2004).

## 2. Materials and Methods

### 2.1. Human and Monkey Tissues

Donor eyes were obtained from the Michigan Eye-Bank within 24 hours of death. The protocol adhered to the provisions of the Declaration of Helsinki for the use of human tissue in research. The tissue was rejected if the donor had a history of ocular disease or if the tissue showed gross abnormalities on visual examination. Monkey (*Macaque fascicularis* or *M. mulatto*) eyes were obtained from National Primate Centers. The globes were hemisected by a circumferential incision around the pars plana. Neural retinas were dissected, snap frozen, and stored at −80° C until use. After neural retina removal, RPE sheets were enzymatically isolated as previously described (Buraczynska et al., 2002; Yang et al., 2003) and examined by phase-contrast microscopy to determine their integrity and confirm the absence of contaminating cells from the neurosensory retina and choroid. Isolation of the RPE from the neural retina was also confirmed by the failure to detect rhodopsin (as a photoreceptor marker) expression in the RPE preparations after 35 PCR cycles in RT-PCR analysis. RPE sheets and neural retinas were snap frozen, and stored at −80°C until use.

### 2.2. Total RNA Isolation

Total RNA was isolated from pooled human RPE sheets (for conventional RT-PCR analysis), or RPE sheets from individual donors (for real-time RT-PCR analysis) using Trizol reagent (Life Technologies, Inc., Rockville, MD) following the manufacturer's instructions. The concentration of total RNA was measured by ultraviolet spectrophotometry or fluorimetry (RediPlate™ 96 RiboGreen® RNA assay, Molecular Probes, Eugene, OR). The quality of each

RNA preparation was checked by denaturing formaldehyde agarose gel electrophoresis, and only those showing intact 28S and 18S ribosomal RNA bands were used for further analysis. Human retinal RNA was isolated and measured following the procedures described above. Human heart and kidney total RNAs were purchased from Clontech (Palo Alto, CA).

### 2.3. PCR Primers

The primers and expected sizes of RT-PCR products for human Kir7.1, its splice variant Kir7.1S, glyceraldehyde-3-phosphate dehydrogenase (GAPDH; as the endogenous control or reference), and rhodopsin are shown in Table 1. As Kir7.1 primer sets 1 and 2 were designed to span an intron of 2089 bp, products from genomic DNA could be readily distinguished from products resulting from cDNA amplification.

### 2.4. Conventional RT-PCR Analysis

Total RNA was treated with DNase I (DNAfree; Ambion, Austin, TX) and reverse transcribed with random decamers using reverse transcriptase (RETROscript™; Ambion, Austin, TX) following procedures outlined in the manufacturer's instructions. PCR was performed with gene- or splice variant-specific primer sets (Table 1). The PCR products were generated by adding DNA polymerase (Taq DNA polymerase; Gibco BRL Life Technologies, Gaithersburg, MD or SuperTaq-Plus™; Ambion, Austin, TX) and cycled 30 times for GAPDH or 35 times for Kir7.1, Kir7.1S, or rhodopsin (1 min at 94°C, 1 min at 54°C–64°C, 0.5 –1 min at 72°C), followed by a 7 min-extension at 72°C. The RT-PCR products were separated by 1.5% agarose gel electrophoresis.

### 2.5. Real-time PCR Analysis

The expression of Kir7.1 and Kir7.1S in human RPE was quantified by SYBR Green I real-time PCR assay on a thermal cycler (iCycler iQ; Bio-Rad Laboratories, Hercules, CA). The real-time PCR conditions were optimized in preliminary experiments. The following master mix of the components was prepared to the indicated end-concentrations: samples (diluted synthesized cDNA corresponding to 1–100 ng total RNA), forward primer (0.25 μM), reverse primer (0.25 μM) and 1 × SYBR Green Supermix (Bio-Rad Laboratories, Hercules, CA). An aliquot of 25 μl was dispensed into each well of a 96-well optical plate. The following PCR cycle parameters were used: an initial denaturation step and hot-start iTaq DNA polymerase activation (95°C for 3 min) followed by 40 cycles of denaturation (94°C for 30 s) and annealing/extension (63.9°C for 60 s). Fluorescence data were acquired during the annealing/extension step. The data were analyzed with iCycler™ iQ optical system software (version 3.0a; Bio-Rad Laboratories, Hercules, CA) and a fractional cycle number at which a threshold fluorescence was obtained (threshold cycle, $C_T$). To confirm amplification specificity, the PCR products from each primer pair were subjected to melting curve analysis and subsequent 2.0% agarose gel electrophoresis. Melting curve analysis was carried out as follows: 95°C for 1 min, 55°C for 1 min, followed by a temperature increase of 0.5°C to 95°C. Fluorescence was measured continually during this melting curve cycle.

### 2.6. Quantitative Analysis of Kir7.1 and Kir7.1S Expression

Kir7.1 and Kir7.1S mRNA levels were quantified using the relative standard curve method, as described in Applied Biosystems User Bulletin No. 2 (P/N 4303859). Briefly, standard curves with known amounts of total RNA pooled from human neural retina, kidney, and heart were generated for the target (Kir7.1 and Kir7.1S) and reference (GAPDH). Threshold cycle ($C_T$) was plotted against log (ng of total RNA) and the parameters (slope and y-intercept) of the Kir7.1, Kir7.1S and GAPDH curves were calculated by linear regression analysis. The relative amounts of Kir7.1 and Kir7.1S mRNA from RPE samples were calculated from their respective standard curves. These values were then divided by the relative amounts of GAPDH quantified

in the same way from the GAPDH standard curve. The amplification efficiencies for Kir7.1, Kir7.1S and GAPDH were 0.97, 0.92 and 1.00, respectively.

### 2.7. PCR of Genomic DNA

Human genomic DNA was purchased from Clontech (Palo Alto, CA). For Kir7.1 and Kir7.1S primer sets 1 & 2 (see Table 1), the PCR products were generated by adding DNA polymerase (AccuTaq LA DNA polymerase; Sigma, St. Louis, MO) and cycled 30 times (15 seconds at 94°C, 20 seconds at 52°C, 4 minutes at 68°C), followed by a 10 min-extension at 68°C. The PCR products were separated by 1.2% agarose gel electrophoresis. For Kir7.1-specific primer set 3 and Kir7.1S-specific primer set 4, PCR reactions were performed in the same way as described above for human RPE cDNA. The amount of genomic DNA used in each reaction was 100 ng.

### 2.8. DNA Sequencing and Bioinformatic Analysis

RT-PCR fragments were gel purified with QIAquick gel extraction kit (Qiagen, Valencia, CA), measured by ultraviolet spectrophotometry or fluorimetry (RediPlate™ 96 PicoGreen® dsDNA assay kit, Molecular Probes, Eugene, OR) and directly confirmed by bi-directional sequencing with the same sets of primers used for PCR. DNA sequencing was performed by the DNA Sequencing Core Facility at the University of Michigan. The cDNA sequences of amplicons were compared to published sequences using Lasergene software (DNASTAR, Madison, WI). Exons and introns of *KCNJ13* were determined by comparing published genomic DNA sequence with Kir7.1 and Kir7.1S cDNA sequences using Lasergene software (DNASTAR) and by searching AceView (www.humangenes.org).

### 2.9. Cloning of Human Kir7.1S

Human Kir7.1S was amplified by PCR from human RPE cDNA (reverse transcribed as described above) using primers designed according to the Kir7.1S RT-PCR product sequence (see Fig. 2A) (sense primer, 5′-GAG ATG GAC AGC AGT AAT TGC AAA G -3′; antisense primer: 5′-ACT ACT GCT GTG TCA GTA AAG CG -3′). The RT-PCR product was TA-cloned into pcDNA3.1 (Invitrogen, San Diego, CA) for expressional studies in *Xenopus* oocytes. The reading frame and orientation of the insert were confirmed by DNA sequencing.

### 2.10. Western Blot Analysis

Protein preparation and Western blot analysis were performed using the techniques described previously (Greering et al., 1989; Zhang et al., 2005) with minor modifications. Briefly, native human RPE sheets were placed into buffer A (150 mM NaCl, 20 mM Tris- HCl [pH 7.4], 2 mM EDTA, 2% sodium dodecyl sulfate (SDS) containing complete protease inhibitor cocktail (Pierce Rockford, IL), and 10 mM 2-mercaptoethanol) and homogenized. Homogenized samples were centrifuged at 15,000 *g* for 10 minutes at room temperature and the supernatants collected. Oocytes were homogenized in buffer containing 83 mM NaCl, 1 mM $MgCl_2$, 10 mM 4-(2-hydroxyethyl)piperazine-1-ethanesulfonic acid (HEPES), pH 7.0, and complete protease inhibitor cocktail and centrifuged at 1,000 *g* to remove yolk. The resulting supernatant was centrifuged at 165,000 *g* for 90 minutes to produce a microsomal pellet, which was solubilized in buffer A. Proteins were mixed in Laemmli sample buffer (62.5 mM Tris [pH 6.8], 25% glycerol, 2% SDS, 0.01% bromophenol blue, and 5% 2-mercaptoethanol; Bio-Rad, Hercules, CA). One μg of microsome protein from oocytes and 10 μg of protein extract from human RPE were applied to 4% to 20% linear gradient Tris-HCl gel (Bio-Rad). After electrophoresis, proteins were transferred to a polyvinylidene difluoride (PVDF) membrane (Bio-Rad) at a constant current of 250 mA for 60 minutes at 4°C in a solution containing 25 mM Tris, 193 mM glycine, and 10% methanol. The membrane was then incubated at room temperature first with Tris-buffered saline containing 5% nonfat-dried milk and 0.1% Tween

20 and then with anti-Kir 7.1 antibody (sc-22438, Santa Cruz Biotechnology, Santa Cruz, CA) pre-incubated with or without antigenic peptide in the same solution. Immune complexes were detected with horseradish peroxidase –conjugated secondary antibodies and enhanced with chemiluminescent substrate (Pierce, Rockford, IL).

### 2.11. Functional Assessment of Human Kir7.1S Expressed in Xenopus oocytes

Capped poly-$A^+$ cRNA was synthesized from linearized transcription plasmid cDNA containing the coding region of human Kir7.1 (pBSTA expression vector) or Kir7.1S (pcDNA3.1) using a commercially available cRNA capping kit (Ambion Inc., Austin, Texas). cRNA was precipitated in ethanol, dried, and re-dissolved in DEPC-treated water.

All procedures with animals were designed to minimize pain and suffering and conformed to the ARVO Statement for the Use of Animals in Ophthalmology and Vision Research. *Xenopus laevis* oocytes were surgically removed from deeply anesthetized adult females as described previously (Shimura et al., 2001). Healthy-looking stage V-VI oocytes were defolliculated, injected with 10 ng of human Kir7.1 cRNA, Kir7.1S cRNA, or 10 ng of each cRNA in 50 nl DEPC-treated water, and maintained at 18 °C in incubation solution (96 mM NaCl, 2 mM KCl, 1 mM $CaCl_2$, 1 mM $MgCl_2$, 10 mM HEPES (pH 7.4), 300 mg/ml gentamicin, and 550 mg/ml sodium pyruvate) for up to 72 hr before recording.

Whole-cell currents were recorded in oocytes using the two-electrode voltage-clamp technique as described previously (Shimura et al., 2001; Yang et al., 2000). The standard bathing solution was ND96 (96 mM NaCl, 2 mM KCl, 10 mM Na-HEPES, 1.0 mM $CaCl_2$, and 1.0 mM $MgCl_2$, pH 7.4). Permeation properties of the channels were assessed by replacing ND96 with 98 mM $K^+$ or 98 mM $Rb^+$ solutions, which were identical in composition to ND96 except that NaCl was replaced by 96 mM KCl or NaCl and KCl were replaced by RbCl.

### 2.12. Statistical analysis

All statistical analyses were performed using the unpaired Student's *t*-test. Data are expressed as mean ± standard error. A value of $P < 0.05$ was considered statistically significant.

## 3. Results

### 3.1. Identification of Kir7.1S

Using primer pairs designed to amplify an 813-bp length of human Kir7.1 (primer set 1, Table 1), we detected two bands in PCR analysis of reverse transcribed mRNA isolated from the RPE and retina of adult human donor eyes. As shown in Fig. 1A (lane 1), the upper band was the predicted size for the Kir7.1 product (813-bp), and sequencing revealed that it was identical to the published human Kir7.1 cDNA sequence (GenBank accession no. **AB013891**). The lower band (577-bp) was also purified and sequence analysis revealed that this product was identical to the 813-bp fragment except for a 236-bp deletion. We designated this sequence Kir7.1 short, or Kir7.1S. Using the same primer pair, we also found expression of Kir7.1 and Kir7.1S in human neural retina (Fig. 1A, lane 3) and in monkey RPE and neural retina (Fig. 1B). We also detected Kir7.1 and Kir7.1S in human kidney and brain (Fig. 1C), where Kir7.1 expression has also been reported (Nakamura et al., 1999,2000;Ookata et al., 2000).

To determine whether there might be additional sequence differences between the two transcripts, the full coding sequence of Kir7.1 was amplified using another set of primers (primer set 2, Table 1). Again, two bands were amplified, an upper band with the predicted size for Kir7.1 (1217 bp) and a lower 981-bp band (Fig. 1D). The two bands were excised, purified and sequenced. Sequencing indicated that the 981-bp RT-PCR product was identical to the 1217-bp product except for a 236-bp deletion. Figure 2A compares the nucleotide

sequences of these 1217- and 981-bp products. The 1217-bp Kir7.1 cDNA contained the entire coding sequence, with its 1083-bp open reading frame (ORF) located between positions 20 and 1102. The 981-bp Kir7.1S cDNA encoded a partial untranslated 19-bp 5′ region, a 285-bp ORF, and an untranslated 677-bp 3′ region. The 236-bp deletion starts at a position corresponding to 244 of the Kir7.1 cDNA and results in a translation frame shift that introduces a stop codon at a position corresponding to position 538 of Kir7.1.

The putative Kir7.1S protein contains 94 amino acid residues (predicted molecular weight, 11 kDa), with the first 75 amino acid residues being identical to a region of Kir7.1 comprising the N-terminus and most of M1 (Fig. 2B). At the C-terminus, Kir7.1S has a stretch of 19 residues that are not present in Kir7.1.

### 3.2. Kir7.1S mRNA is generated by alterative splicing of Kir7.1 pre-mRNA

To test the possibility that Kir7.1S mRNA is transcribed by a “Kir7.1-like” gene distinct from the *KCNJ13*, genomic DNA from human blood was used as template for PCR with primer sets that were successful in amplifying Kir7.1 and Kir7.1S from human RPE cDNA. Although a product of the predicted size for *KCNJ13* was successfully amplified with primer set 1 (predicted size: 2902 bp; Fig. 3A, lane 1) or set 2 (predicted size: 3306 bp; Fig. 3A, lane 3), no secondary product was detected under either condition. A band of the correct size (170 bp) for *KCNJ13* was also successfully amplified when Kir7.1-specific primer set 3 was used (Fig. 3B, lanes 1 & 2), but no product of 173 bp was amplified when Kir7.1S-specific primer set 4 was used (Fig. 3B, lanes 4 & 5). This indicates that a distinct gene encoding the short form of Kir7.1 (Kir7.1S) does not exist within the human genome and that instead the Kir7.1S transcript detected in human RPE by RT-PCR is generated by the alternative splicing of Kir7.1 pre-mRNA.

To determine how Kir7.1 pre-mRNA might be alternatively spliced, we performed a BLAST search of the GenBank nucleotide database with the RPE Kir7.1 and Kir7.1S cDNA sequences and obtained alignments with a published human Kir7.1 cDNA sequence (GenBank accession no. **NM_002242**) as well as the reverse strand of *Homo sapiens* BAC clone RP11-174L18 from chromosome 2 (GenBank accession no. **AC064852**). A comparison of these sequences and information obtained from AceView (www.humangenes.org) revealed that *KCNJ13* contains 3 exons, 2 introns, and spans 10,114 bp of genomic DNA (Fig. 4A). Further data analysis identified a 5066-bp intron in the untranslated 5′ region (intron 1) and a novel alternative donor splice site within the second exon. The production of Kir7.1 and Kir7.1S transcripts results from alternative usage of two competing 5′ splice (donor) sites. The usage of the proximal 5′ splice site gives rise to a transcript encoding full-length Kir7.1, while selection of the distal 5′ splice site produces a shortened transcript, Kir7.1S, which lacks the 236-bp sequence of exon 2b (Fig. 4A). Sequence analysis revealed that both Kir7.1 and Kir7.1S have conserved consensus sequences at the 5′ and 3′ intronic splice sites, i.e., the presence of GT at the 5′ splice site and AG at the 3′ splice site (Fig. 4B).

### 3.3. Quantification of Kir7.1 and Kir7.1S mRNA

Kir7.1 and Kir7.1S transcripts detected by conventional RT-PCR were selected for further analysis by real-time RT-PCR to determine their relative abundance. Total RNA was extracted from RPE sheets isolated from individual donors and treated with DNase I to remove any residual genomic DNA. cDNA was reverse transcribed from individual donors’ RPE RNA and used as template for real-time PCR with primers specific for Kir7.1, Kir7.1S, or GAPDH (Table 1). Figure 5, A–C, shows the results of a representative experiment using primers specific for Kir7.1, Kir7.1S, or GAPDH. Figure 5A shows that fluorescence threshold was reached after 21.2 cycles for Kir7.1 and 23.2 cycles for Kir7.1S, compared to 20.3 cycles for GAPDH. This indicates that Kir7.1 transcript is nearly as abundant as GAPDH mRNA and that Kir7.1S

transcript is expressed at a lower level. The specificities of Kir7.1, Kir7.1S, and GAPDH RT-PCR products were confirmed by melting curve analysis, which showed single product-specific melting temperature peaks in each case (Fig. 5B). Furthermore, agarose gel electrophoresis of the RT–PCR products yielded single product bands of the expected size (Fig. 5C). The relative quantities of Kir7.1 and Kir7.1S mRNAs in the RPE were calculated using the relative standard curve method (see Methods) in which GAPDH served as the endogenous control. Figure 5D summarizes the relative expression of Kir7.1 and Kir7.1S in the native RPE obtained from the five donors and shows that Kir7.1S transcript is expressed at a 4-fold lower level than Kir7.1 transcript ($P < 0.01$).

### 3.4. Kir7.1S protein expression

To determine whether Kir7.1S message can be translated into protein, Kir7.1S cRNA was injected into *Xenopus* oocytes. Proteins from Kir7.1S cRNA-injected oocytes were solubilized in Laemmli sample buffer followed by SDS-PAGE and transferred to PVDF membranes. The PVDF blots were probed with an affinity-purified polyclonal anti-Kir7.1 antibody raised against a synthetic peptide corresponding to amino acid residues at the N-terminus of human Kir7.1. This Kir7.1 N-terminal antibody is expected to recognize both Kir7.1 and Kir7.1S because the N-termini of these two proteins are predicted to be identical. Figure 6 shows that a single band of ~11 kDa was detected specifically on the blot of proteins from Kir7.1S cRNA-injected oocytes (left panel, lane 2). The band correspond to Kir7.1S because, first, it was about the predicted size of 11 kDa for unmodified Kir7.1S and, second, it was not detected on the blot of proteins from uninjected oocytes (left panel, lane 1), or on the blot of proteins from Kir7.1S cRNA-injected oocytes after pre-absorption of the antibodies with antigenic peptide (right panel, lane 2). These results are representative of 10 similar experiments.

To test for the presence of Kir7.1S protein in native human RPE cells, we performed Western blot analysis on a blot of lysate from human RPE sheets. Figure 6 shows that this antibody immunolabeled a single band of ~50 kDa corresponding to Kir7.1 (left panel, lane 3). The identity of the labeled protein band as Kir7.1 was confirmed by the elimination of staining when the anti-Kir7.1 antibody was preincubated with the synthetic Kir7.1 N-terminal peptide (Fig. 6, right panel, lane 3). No band of the size predicted for Kir7.1S was detected. Similar results were obtained in 3 other experiments.

### 3.5. Functional assessment of Kir7.1S expressed in Xenopus oocytes

Because its predicted peptide sequence lacks the $K^+$ selectivity sequence and much of the pore-lining regions of Kir7.1, the Kir7.1S subunit is not expected to be capable forming functional homotetrameric channels. It is conceivable, however, that Kir7.1S could co-assemble with Kir7.1 channel subunits and alter Kir7.1 channel properties or surface expression (Yamada et al., 2002; Tian et al., 2006). To test this possibility, we injected *Xenopus* oocytes with Kir7.1S cRNA alone or together with Kir7.1 cRNA and recorded whole-cell currents 2 to 3 days later. As expected, oocytes injected with Kir7.1S cRNA alone exhibited currents that were indistinguishable from endogenous *Xenopus* oocyte currents (not shown). Oocytes injected with Kir7.1 cRNA resulted in a mildly inwardly rectifying $K^+$ current that displayed a low dependence of conductance on extracellular $K^+$ (Fig. 7A) but a high dependence on extracellular $Rb^+$ (Fig. 7B), reflecting the unusual permselectivity of this Kir channel subtype (Doring et al., 1998; Wischmeyer et al., 2000; Shimura et al., 2001). When Kir7.1S cRNA was co-injected with Kir7.1 cRNA, the whole-cell current exhibited rectification and dependence on $K^+$ and $Rb^+$ that was essentially identical to that obtained in oocytes injected with Kir7.1 cRNA alone (Figs. 7C and 7D). The amplitudes of $K^+$ and $Rb^+$ currents in Kir7.1:Kir7.1S co-injected oocytes tended to be somewhat larger than those in oocytes injected with Kir7.1 alone, but these differences were not statistically significant ($P>0.10$). These results indicate that Kir7.1S has no functional interaction with Kir7.1.

## 4. Discussion

A major finding of this paper is that the human RPE expresses both full-length Kir7.1 and a novel truncated splice variant, Kir7.1S. Although the expression of other alternative splice variants of Kir7.1 in rat small intestine and testis has been reported (Nakamura et al., 2000), those variants are generated by various combinations of non-coding exons. In contrast, Kir7.1S involves alternative splicing of exon 2, which encodes the N-terminus and most of the two membrane spanning domains. Previously, Derst *et al.* (1998) identified a single intron within the coding region of *KCNJ13* and suggested that there may be an intron in the non-coding 5′ region; the analysis in present study confirms both of these features of the human Kir7.1 gene structure. More importantly, our analysis identified an alternative donor splice site within the second exon that gives rise to Kir7.1S. Human Kir7.1 pre-mRNA splicing links one of two alternative 5′ (donor) splice sites to a single 3′ (acceptor) splice site to produce either Kir7.1 or Kir7.1S. Kir7.1S mRNA is homologous to Kir7.1 but it is deficient by 236 bp, leading to a translation frame shift and the introduction of stop codon. Consequently, the predicted protein is truncated, consisting of the N-terminus and most of the first transmembrane domain of the Kir7.1 subunit.

The expression of Kir7.1S mRNA is not limited to human RPE but was also detected in human neural retina, kidney, brain, as well as in monkey RPE and neural retina. This indicates that the expression of Kir7.1S is conserved. Using an antibody against the N-terminal of human Kir7.1, we demonstrated the translation of Kir7.1S in the *Xenopus* oocyte expression system. In native human RPE, however, we found evidence only for the expression of full-length Kir7.1. The absence of detectable levels of Kir7.1S suggests that this protein may be rapidly degraded in normal human RPE. Kir channels are formed by the co-assembly of four identical or structurally related subunits, each of which consists of two membrane spanning domains (M1 and M2) and an intervening pore loop (H5) that contains the potassium selectivity filter. In addition, some Kir channels, notably members of the Kir1 and Kir6 subfamilies, assemble with β subunits (SUR). Because the predicted Kir7.1S protein lacks the regions that compose the channel pore in the full-length subunit (H5, M2, and C-terminus), it is improbable that it alone could form a functional channel. It seemed possible, however, that Kir7.1S might be capable of altering the expression, stability, or trafficking of Kir7.1, or the functional properties of the Kir7.1 channel (Yamada et al., 2002; Tian et al., 2006). Evidence against these types of interaction between Kir7.1S and Kir7.1 was obtained in electrophysiological experiments, which showed no significant effect on Kir7.1 current amplitude, rectification, or cation permselectivity in *Xenopus* oocytes when Kir7.1S cRNA was co-injected with Kir7.1 cRNA. These biophysical results suggest that there is no functional interaction between Kir7.1S and Kir7.1 proteins. It is also possible that when both variants are co-expressed in oocytes, Kir7.1S is degraded at a higher rate than when expressed alone.

In summary, the present study confirms the expression of Kir7.1 in human RPE and provides the first identification of a Kir7.1 splice variant resulting in predicted changes in amino acid sequence. Our study demonstrates that: (1) Kir7.1S transcript is expressed in human RPE as well as several other human tissues expressing Kir7.1, including retina, kidney, and brain; (2) Kir7.1S transcript in the RPE is expressed at a moderate level, approximately 4-fold lower than that of Kir7.1 transcript; and (3) although Kir.7.1S is translated into protein in *Xenopus* oocytes, it does not appear to interact functionally with Kir7.1. It is possible that pre-mRNA splicing regulation could play an important role in determining the relative abundance of Kir7.1 and Kir7.1S mRNAs and, hence, Kir7.1 channel density.

## Acknowledgments

This work was supported by NIH Grant EY08850, Core Grant EY07703, the Foundation Fighting Blindness and RPB Lew R. Wasserman Merit Award to BAH. The authors thank the Michigan Eye Bank (Ann Arbor, MI) for assistance in obtaining human eye tissues and Dr. David M. Reed for help in acquiring AceView information.

## References

Buraczynska M, Mears AJ, Zareparsi S, et al. Gene expression profile of native human retinal pigment epithelium. Invest Ophth Vis Sci 2002;43:603–607.

Derst C, Doring F, Preisig-Muller R, et al. Partial gene structure and assignment to chromosome 2q37 of the human inwardly rectifying $K^+$ channel (Kir7.1) gene (*KCNJ13*). Genomics 1998;54:560–563. [PubMed: 9878260]

Doring F, Derst C, Wischmeyer E, et al. The epithelial inward rectifier channel Kir7.1 displays unusual K+ permeation properties. J Neurosci 1998;8:8625–8636. [PubMed: 9786970]

Geering K, Theulaz I, Verrey F, Häuptle MT, Rossier BC. A role for the beta-subunit in the expression of functional $Na^+$-$K^+$-ATPase in *Xenopus* oocytes. Am J Physiol 1989;257:C851–C858. [PubMed: 2556932]

Hughes BA, Steinberg RH. Voltage-dependent currents in isolated cells of the frog retinal pigment epithelium. J Physiol 1990;428:273–297. [PubMed: 2231414]

Hughes BA, Shaikh A, Ahmad A. Effects of $Ba^{2+}$ and $Cs^+$ on apical membrane $K^+$ conductance in toad retinal pigment epithelium. Am J Physiol 1995;268:C1164–C1172. [PubMed: 7762609]

Hughes BA, Takahira M. Inwardly rectifying $K^+$ currents in isolated human retinal pigment epithelial cells. Invest Ophthal Vis Sci 1996;37:1125–1139. [PubMed: 8631627]

Hughes BA, Takahira M. ATP-dependent regulation of inwardly rectifying $K^+$ current in bovine retinal pigment epithelial cells. Am J Physiol 1998;275:C1372–C1383. [PubMed: 9814987]

Isomoto S, Kondo C, Kurachi Y. Inwardly rectifying potassium channels: their molecular heterogeneity and function. Jpn J Physiol 1997;47:11–39. [PubMed: 9159640]

Kusaka S, Inanobe A, Fujita A, et al. Functional Kir7.1 channels localized at the root of apical processes in rat retinal pigment epithelium. J Physiol 2001;531:27–36. [PubMed: 11179389]

Nakamura N, Suzuki Y, Sakuta H, Ookata K, Kawahara K, Hirose S. Inwardly rectifying $K^+$ channel Kir7.1 is highly expressed in thyroid follicular cells, intestinal epithelial cells and choroid plexus epithelial cells: implication for a functional coupling with $Na^+$, $K^+$-ATPase. Biochem J 1999;342:329–336. [PubMed: 10455019]

Nakamura N, Suzuki Y, Ikeda Y, Notoya M, Hirose S. Complex structure and regulation of expression of the rat gene for inward rectifier potassium channel Kir7.1. J Biol Chem 2000;275:28276–28284. [PubMed: 10871613]

Ookata K, Tojo A, Suzuki Y, Nakamura N, Kimura K, Wilcox CS, Hirose S. Localization of inward rectifier potassium channel Kir7.1 in the basolateral membrane of distal nephron and collecting duct. J Am Soc Nephrol 2000;11:1987–1994. [PubMed: 11053473]

Shimura M, Yuan Y, Chang JT, et al. Expression and permeation properties of the $K^+$ channel Kir7.1 in the retinal pigment epithelium. J Physiol 2001;531:329–346. [PubMed: 11230507]

Tian W, Fu Y, Wang DH, Cohen DM. Regulation of TRPV1 by a novel renally expressed rat TRPV1 splice variant. Am J Physiol Renal Physiol 2006;290:F117–126. [PubMed: 16091583]

Yamada Y, Chen X, Kobayashi T, et al. A truncated splice variant of KCNQ1 cloned from rat heart. Biochem Biophys Res Commun 2002;294:199–204. [PubMed: 12051693]

Yang D, Sun F, Thomas LL, et al. Molecular cloning and expression of an inwardly rectifying $K^+$ channel from bovine corneal endothelial cells. Invest Ophth Vis Sci 2000;41:2936–2944.

Yang D, Pan A, Swaminathan A, Kumar G, Hughes BA. Expression and localization of the inwardly rectifying potassium channel Kir7.1 in native bovine retinal pigment epithelium. Invest Ophth Vis Sci 2003;44:3178–3185.

Yang D, Hughes BA. Identification of a novel splice variant of the inwardly rectifying $K^+$ channel Kir7.1 in human retinal pigment epithelium (RPE). Invest Ophth Vis Sci ARVO 2004. 2004Abstract #4717

Yuan Y, Shimura M, Hughes BA. Regulation of inwardly rectifying $K^+$ channels in retinal pigment epithelial cells by intracellular pH. J Physiol 2003;549:429–438. [PubMed: 12665599]

Wischmeyer E, Doring F, Karschin A. Stable cation coordination at a single outer pore residue defines permeation properties in Kir channels. FEBS Lett 2000;466:115–120. [PubMed: 10648824]

Zhang XM, Kimura Y, Inui M. Effects of phospholipids on the oligomeric state of phospholamban of the cardiac sarcoplasmic reticulum. Circ J 2005;69:1116–1123. [PubMed: 16127197]

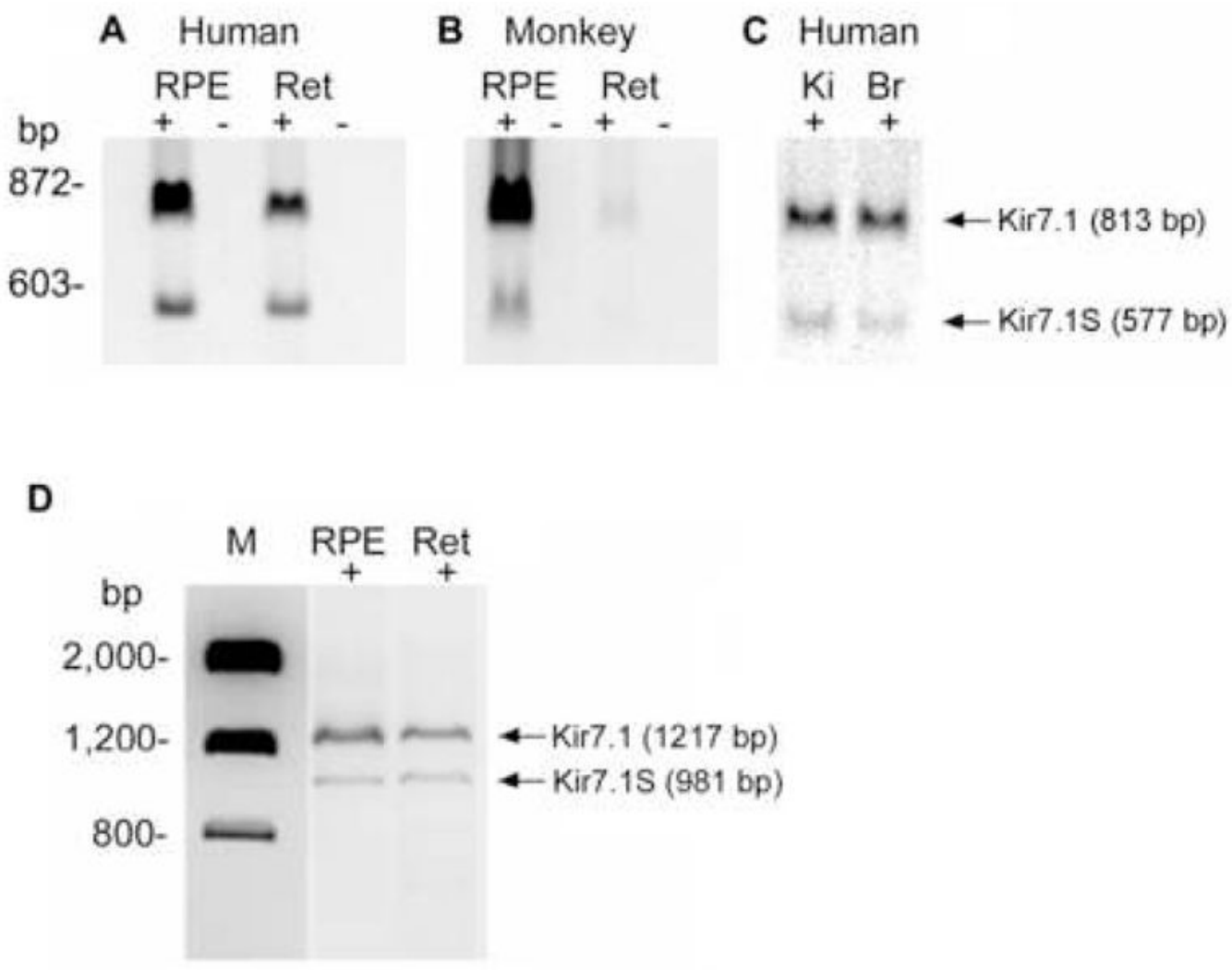


**Figure 1. Expression of Kir7.1 and Kir7.1S in human RPE and other tissues**

Expression of Kir7.1 and Kir7.1S in native human (**A, C, D**) and monkey (**B**) RPE, neural retina (Ret), human kidney (Ki), and brain (Br). RT reactions were performed in the presence (+) or absence (−) of reverse transcriptase. PCR was performed using a primer set specific for both Kir7.1 and Kir7.1S (see Table 1). M: DNA size markers.

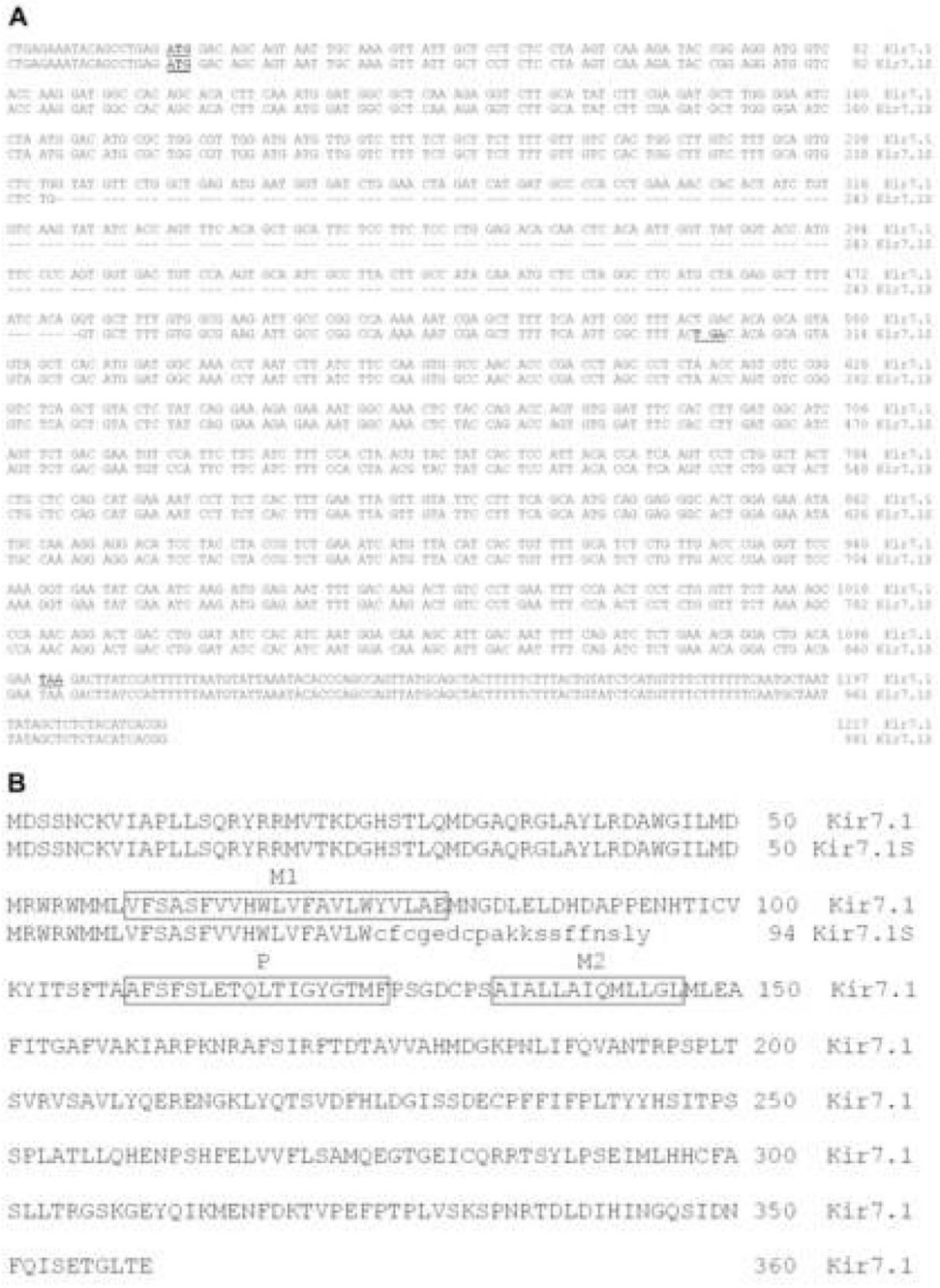


**Figure 2. Kir7.1S nucleotide and protein sequences**

**(A)** Sequences of Kir7.1 and Kir7.1S cDNA derived from native human RPE. Start and stop codons are indicated by bold underlined letters. Deleted region in the Kir7.1S sequence is indicated by short bars. **(B)** Alignment of amino-acid sequences of Kir7.1 and Kir7.1S protein from native human RPE. Lowercase letters indicate differences created by a shift in reading frame for Kir7.1S caused by 236-bp deletion of nucleotides corresponding to 244–479 of Kir7.1 cDNA. M1 and M2 represent two transmembrane segments and P the pore-forming P-region.

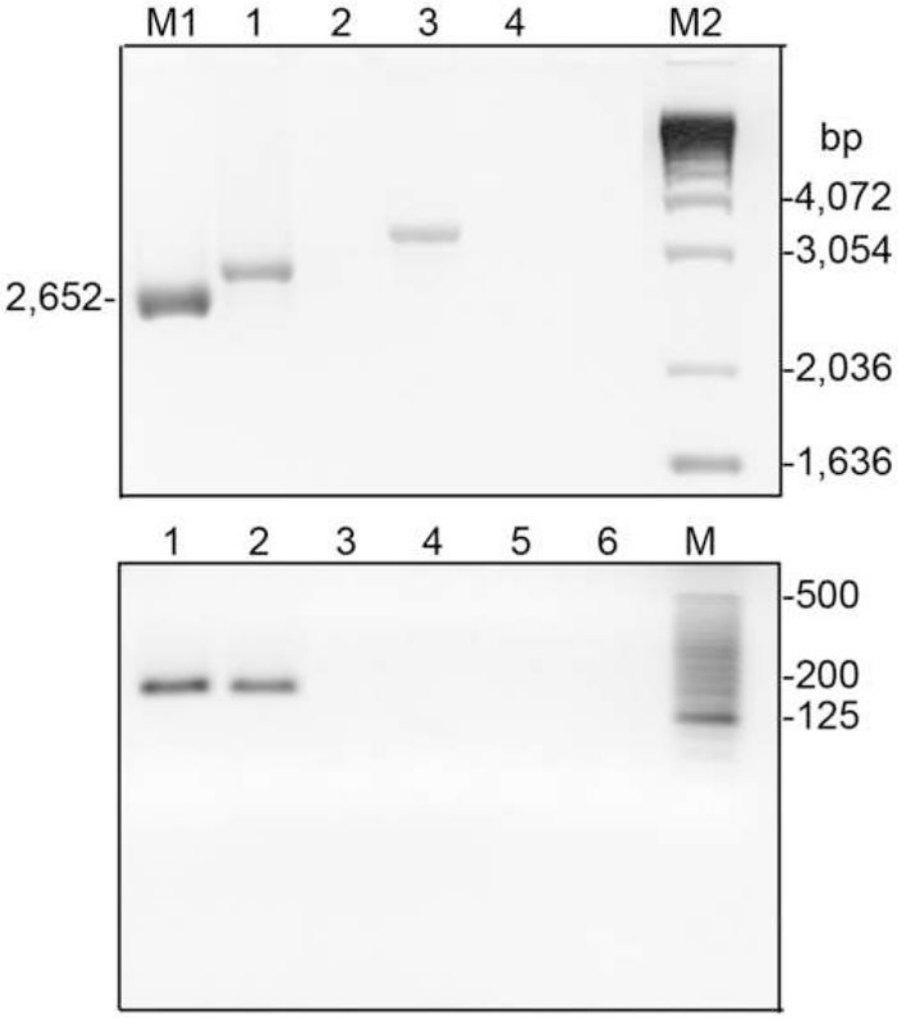


**Figure 3. PCR of human genomic DNA**

PCR was performed with primer set 1 (**A**: lanes 1 & 2), primer set 2 (**A**: lanes 3 & 4), primer set 3 (**B**: lanes 1–3), or primer set 4 (**B**: lanes 4–6) using 100 ng human genomic DNA (**A**: lanes 1 & 3; **B**: lanes 1, 2, 4 & 5) or water (**A**: lanes 2 & 4; **B**: lanes 3 & 6) as template. M1 and M2: DNA size markers. The sizes of the products amplified by primer sets 1, 2, and 3 match those predicted for *KCNJ13*. The failure of Kir7.1S-specific primer set 4 to amplify a product indicates that a distinct gene encoding Kir7.1S does not exist.

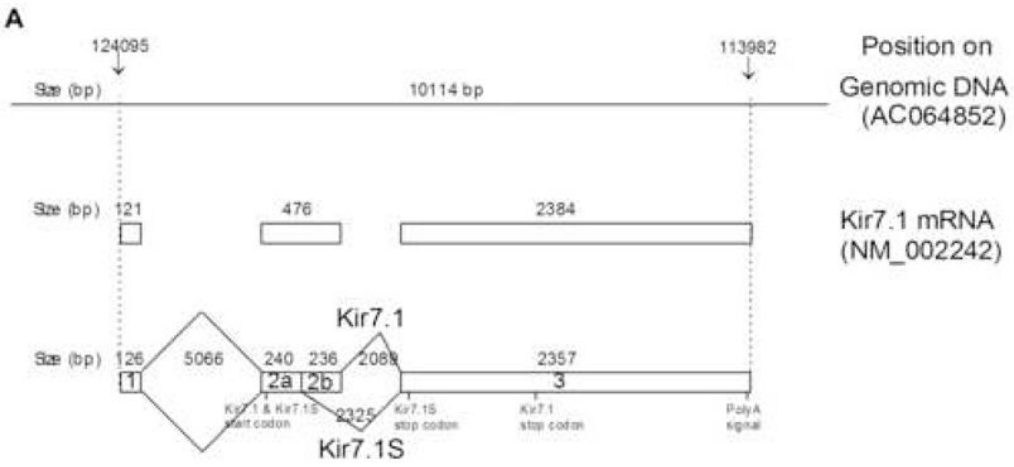


B

| | 5' splice (donor) site | 3' splice (acceptor) site |
|---|---|---|
| Consensus sequence | MAG\|**gt**ragt | **cag**\|G |
| Kir7.1 | CAG\|**gt**aatt (exon 2\|intron 2) | **tag**\|G (intron 2\|exon 3) |
| Kir7.1S | CTG\|**gt**atgt (exon 2\|intron 2) | **tag**\|G (intron 2\|exon 3) |

**Figure 4. The exon-intron organization of human Kir7.1 gene (*KCNJ13*)**

**(A)** The exon-intron organization of human Kir7.1 gene determined by comparing a published human genomic DNA sequence (GenBank accession no. **AC064852**), the Kir7.1 (GenBank accession no. **AY758241**) and Kir7.1S (GenBank accession no. **AY758240**) cDNA sequences revealed in this study, and a published Kir7.1 cDNA sequence (GenBank accession no. **NM_002242**) using Lasergene software (DNASTAR) and information obtained from AceView (www.humangenes.org). Diagonal lines indicate introns and boxes represent exons. The novel alternative donor splice site is located within the second exon. **(B)** Alignment of consensus sequences of splice sites with Kir7.1 and Kir7.1S sequences. Bold lowercase letters indicate GT and AG base pairs for donor and acceptor sites. M represents A or C; r represents a or g.

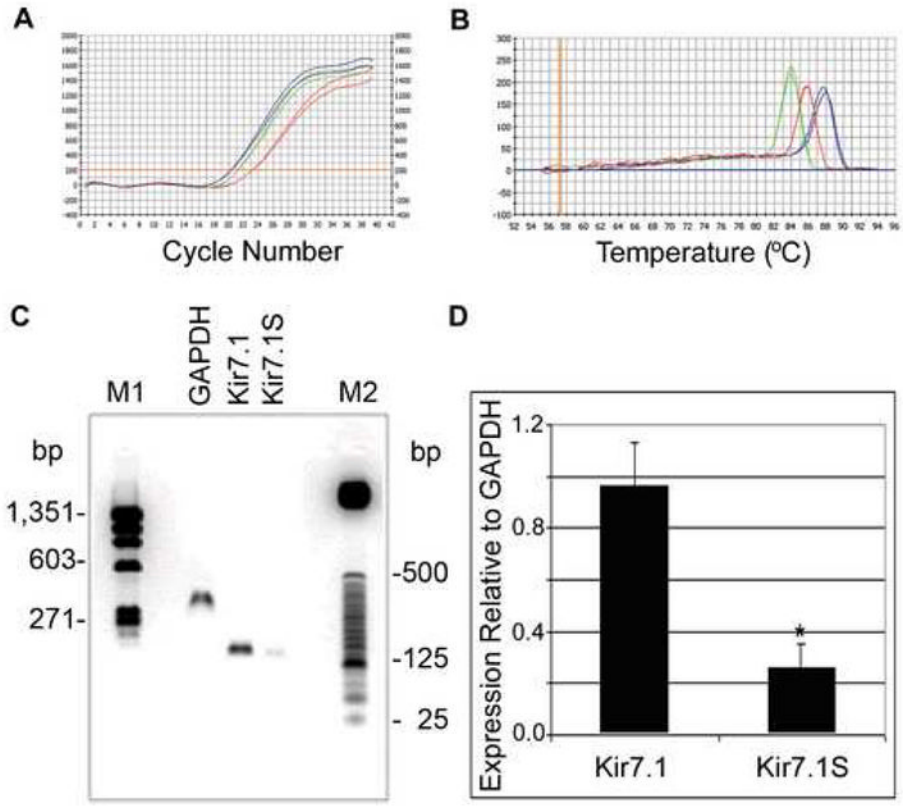


**Figure 5. Quantitation of Kir7.1 and Kir7.1S mRNA levels in native human RPE**

**(A)** Amplification plots of Kir7.1 (green), Kir7.1S (red) and GAPDH (dark blue) in native human RPE. The *y*-axis represents the fluorescence intensity and the *x*-axis the PCR cycle number. **(B)** Melting curves of Kir7.1 (green), Kir7.1S (red) and GAPDH (dark blue). **(C)** Agarose gel electrophoresis of the expression of Kir7.1, Kir7.1S and GAPDH in native human RPE. **(D)** Summary of the relative expression of Kir7.1 and Kir7.1S relative to GAPDH in the RPE obtained from the five donors. **P* < 0.01 compared to Kir7.1.

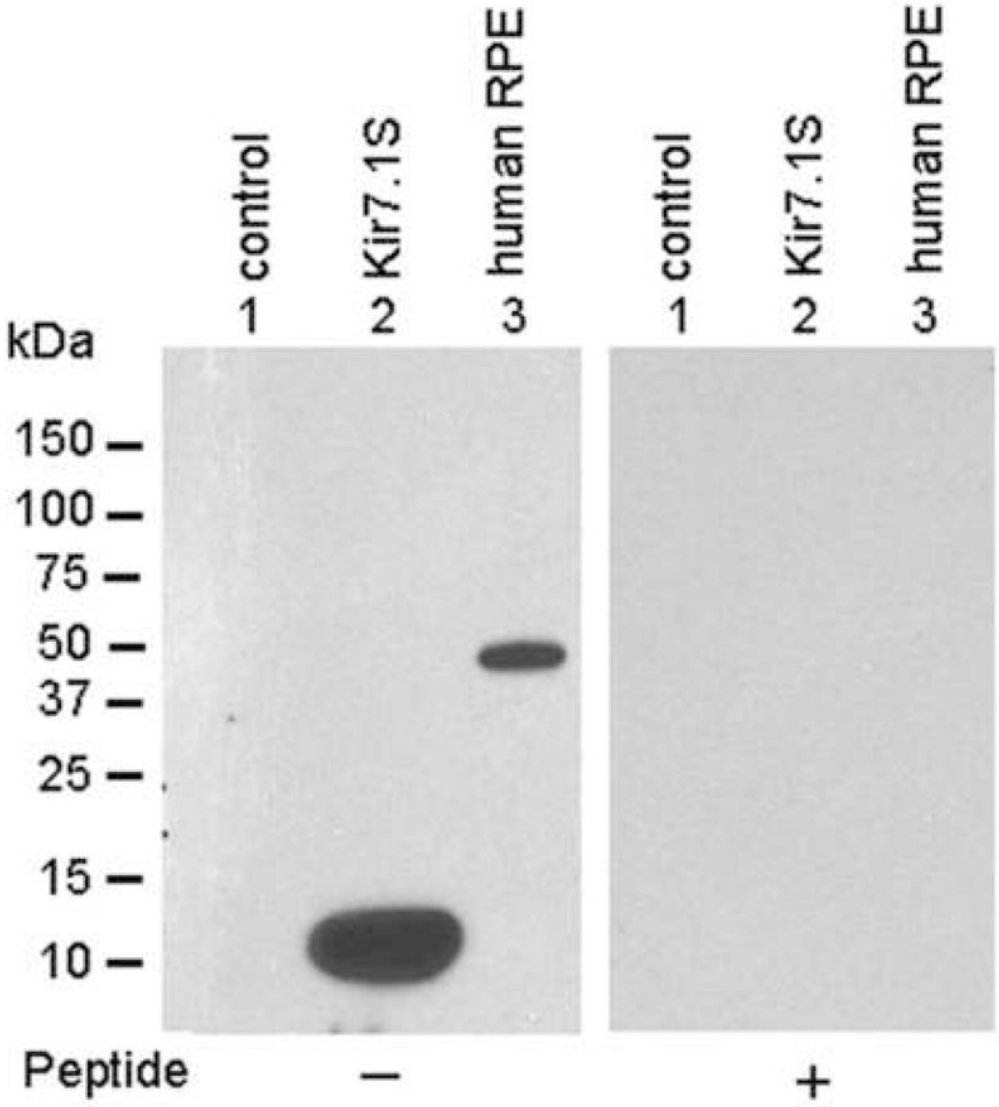


**Figure 6. Expression of human Kir7.1S protein in Kir7.1S cRNA-injected *Xenopus* oocytes and native human RPE**

Western blot of *Xenopus* oocyte protein and human RPE lysate probed with anti-Kir7.1 antibody alone (left panel) or with antibody preabsorbed with antigenic peptide (right panel). *Lane 1*: uninjected *Xenopus* oocytes; *lane 2: Xenopus* oocytes injected with Kir7.1S; and *lane 3*: Native human RPE. Anti-Kir7.1 N-terminal antibody recognized Kir7.1S protein in *Xenopus* oocytes (*lane 2*) but only Kir7.1 in human RPE (lane 3).

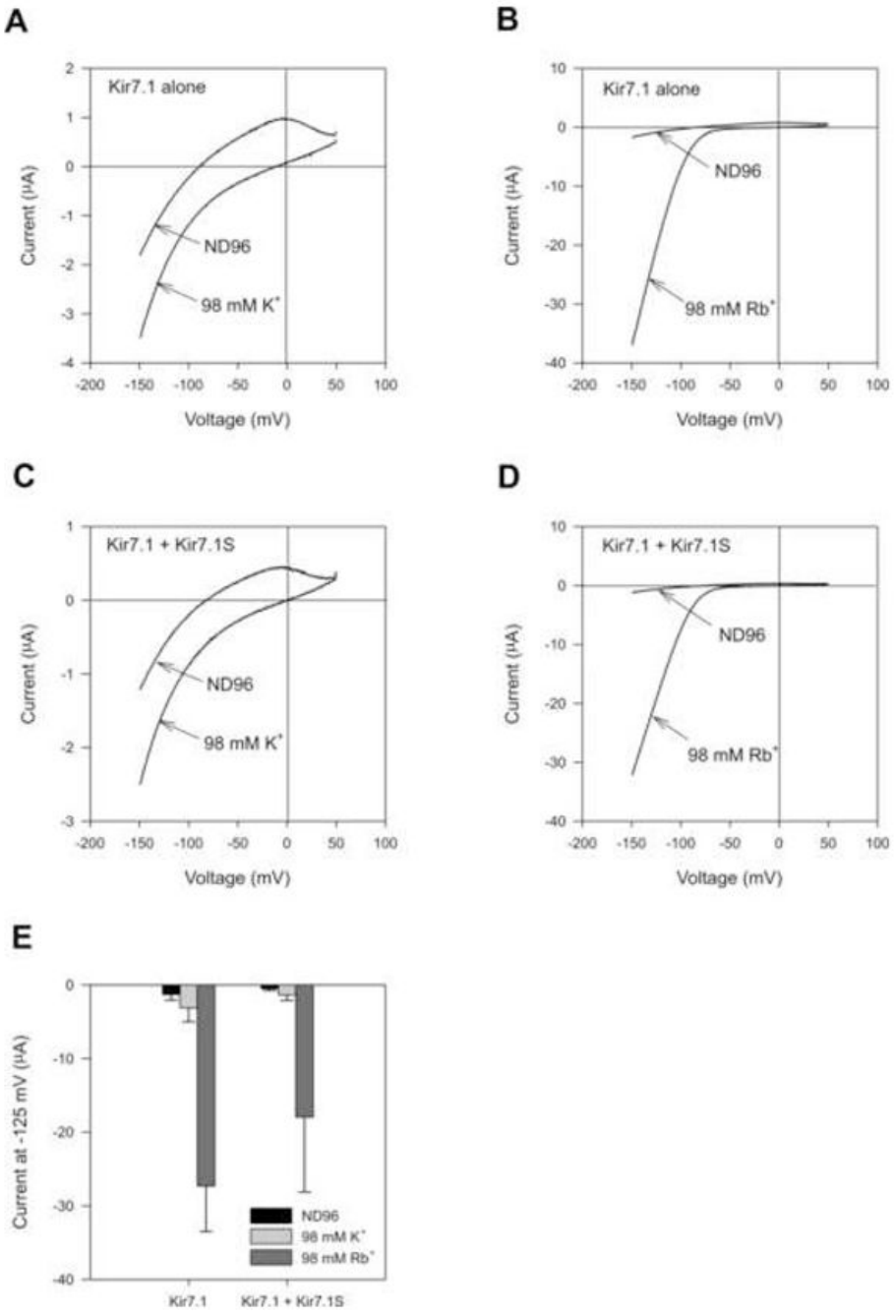


**Figure 7. Functional characterization of Kir7.1 expressed alone and together with Kir7.1S in *Xenopus* oocytes**

Current-voltage (I–V) relationships of whole-cell currents recorded in the presence of extracellular ND96 and 98 mM $K^+$ or 98 mM $Rb^+$ in a Kir7.1 cRNA-injected oocyte (**A** and **B**) and an oocyte injected with equal amounts of Kir7.1 and Kir7.1S cRNAs (**C** and **D**). (**E**) Summary of current amplitudes in Kir7.1- and Kir7.1:Kir7.1S-injected oocytes measured at −125 mV in presence of ND96, 98 mM $K^+$, and 98 mM $Rb^+$ (mean ± SD, n =5 for each group).

**Table 1**

Target gene primer sequences and expected sizes of RT-PCR products

| Target Gene | Sequence | Expected Size (bp) | Position | GenBank Accession# | Note |
|---|---|---|---|---|---|
| **Kir7.1 & Kir 7.1S** | | | | | |
| Set 1(F1/R1) | | 813 for Kir7.1<br>577forKir7.1S | | AB013891 | Used for conventional RT-PCR (cRT-PCR) |
| forward primer: | 5′-TAT CTT CGR GAT GCW TGG GGA AYC -3′ | | 369–392 | | |
| reverse primer: | 5′-YTC ACC TTT GGA ACC TCG KGT C -3′ | | 1181-1160 | | |
| Set 2 (F2/R2) | | 1217 for Kir7.1<br>981 for Kir7.1S | | AB013891 | Used for cRT-PCR<br>*Underlined:* BamH I site |
| forward primer: | 5′-**GCG GGA TC**C TGA GAA ATA CAG CCT G -3′ | | 233–249 | | |
| reverse primer: | 5′-**CGC GGG AT**C CGT GAT GTA GAG AGC -3′ | | 1449-1434 | | *Bold:* added bases |
| **Kir7.1** | | | | | |
| Set 3 (F3/R3) | | 170 | | AB013891 | Used for real-time RT-PCR (rtRT-PCR) |
| forward primer: | 5′-CCC ACC TGA AAA CCA CAC TAT CTG -3′ | | 524–547 | | |
| reverse primer: | 5′-GCA TGA GGC CTA GGA GCA TTT G -3′ | | 693 -672 | | |
| **Kir7.1S** | | | | AY758240 | Used for rtRT-PCR |
| Set 4 (F4/R4) | | 173 | | | |
| forward primer: | 5′-AGG ATG GCC ACA GCA CAC TTC -3′ | | 87–107 | | |
| reverse primer: | 5′-TTC GCC ACA AAA GCA CCA -3′ | | 259-242 | | |
| **GAPDH** | | | | | |
| Set 5 (F5/R5) | | 356 | | AF261085 | Used for rtRT-PCR |
| forward primer: | 5′-GTG AAG GTC GGA GTC AAC G -3′ | | 113–131 | | |
| reverse primer: | 5′-GAG ATG ATG ACC CTT TTG GC -3′ | | 468-439 | | |
| **Rhodopsin** | | | | | |
| Set 6 (F6/R6) | | 577 | | NM_000539 | Used for cRT-PCR |
| forward primer: | 5′-CATCGAGCGGTACGTGGTGGTGTG-3′ | | 491–514 | | |
| reverse primer: | 5′-GCCGCAGCAGATGGTGGTGAGC -3′ | | 1067 - 1046 | | |